

Metrological Array of Cyber-Physical Systems. Part 13. Segmental Approximation for Surface Topology Reconstruction

¹Svyatoslav YATSYSHYN, ¹Bohdan STADNYK, ²Eberhard MANSKE
and ¹Anna KHOMA

¹‘Lviv Polytechnic’ National University, Institute of Computer Technologies, Automation
and Metrology, Bandera str.12, Lviv, 79013, Ukraine

²Ilmenau University of Technology, Department of Production and Precision Metrology,
Gustav-Kirchhoff-Str. 1, D-98693 Ilmenau, Germany

¹Tel.: +38-0322-37-50-89

E-mail: slav.yat@gmail.com

Received: 28 September 2015 /Accepted: 30 November 2015 /Published: 30 December 2015

Abstract: This article presents the segment approximation method for surface topology reconstruction from white light interferogram. The method involves polynomial approximation of separate interferogram segments, and polynomial coefficients are computed at calibration stage. Metrological properties of proposed method are investigated by interferogram modeling tilted and spherical surfaces. *Copyright © 2015 IFSA Publishing, S. L.*

Keywords: White-Light Interferometry, Topology Reconstruction, Mathematical Model, Approximation, Peak Detection, Optical Metrology.

1. Introduction

Measurement of topology or surface profile of objects is important task in many areas, for instance, in medicine [1-2], industry [3-4], scientific researches [5-6]. One of the methods of surface topology measurement is white light interferometry (further - WLI) [6]. Owing to absence of physical contact with researched surface, high resolution and scanning speed, ability to analyze objects of big geometrical size, this technique has been used extensively in tasks of surface research. Moreover WLI unlike monochromatic interferometry enables to measure stepped surfaces and surfaces with significant curvature [7- 8].

Mentioned advantages are wider presented in applications of WLI different techniques for various nanotechnological plants and cyber-physical systems. The most common examples of such usage is measurement of roughness and microstructures profile with nanodimensional Z-resolution, material standards calibration, and also integration with different non-optical measurement techniques for more thorough and versatile analysis of researched object nature [3, 5, 9-10]. For instance, modern 3D profilometer Talysurf CCI 6000 which operates on the basis of WLI and provides surface profile measurement of objects of linear dimension up to several mm with Z-resolution 0.01 nm and XY-resolution 360 nm [11-12].

2. Shortcomings

However the use of white light complicates the analysis of interference signal due to envelope function of Gaussian spectrum [13-14]. Today there are many methods of WLI data processing: fringes tracing, phase shift methods, determination of maximum intensity of interferogram, direct phase demodulation [14-16]. But effectiveness of these methods reduces during complex surfaces reconstruction, especially at analysis of dynamic (variable in time), nonlinear (spherical) surfaces [17]. For this purpose it is urgent to develop new approaches which ensure improvement of metrological characteristics of surface reconstruction methods, and are efficient in realization.

3. Aim of Paper

The goal is the development of precise and accurate computation method of segmental approximation for random topology single-surface reconstruction of interferometric patterns.

4. Mathematical Model of White Light Interferogram

Optical interferometry is non-contact optical method of surface topology determination which is inherent in interference phenomenon.

The interferometer of classical variant includes light source, beam splitter, reference mirror, researched surface and screen (CCD-camera) [7]. The light wave of light source is divided into two paths directed to reference mirror and researched surface respectively. Image is formed in the screen as result of superposition of waves that reflected from respective surfaces. Strengthening and weakening of resultant waves is formed by means of optical difference of light rays paths.

Mathematical model of white-light interferogram is considered in a following way [13]:

$$I(T) = I_0 + E(T) C(T), \quad (1.a)$$

$$E(T) = I_M \cdot \exp\left(-\frac{4 \cdot \Delta\lambda^2 \cdot T^2}{\lambda_0^4}\right), \quad (1.b)$$

$$C(T) = \cos\left(\frac{4 \cdot \pi}{\lambda_0} \cdot T\right), \quad (1.c)$$

where I_0 is the constant component; $E(T)$ represents the interferogram envelope; $C(T)$ denotes the carrier; I_M is the modulation amplitude; T is the optical path difference; λ_0 represents the central wavelength; $\Delta\lambda$ is the spectral bandwidth of the light source.

The sense of reconstruction is to determine the optical path difference T from interferogram that is proportional to height displacement h (or profile) at every point of researched surface:

$$h = \frac{T}{\nu}, \quad (2)$$

where ν is the refractive index.

5. Interferograms Analysis for Different Surfaces

We study the tilted and spherical surfaces that are shown in Fig. 1. The first one is used in measurement of small inclination angles of flat objects (wedge) [18], and spherical surface corresponds to membrane model in pressure sensors [1].

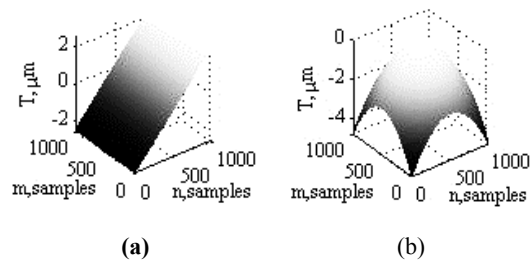


Fig. 1. The tilted (a) and spherical (b) surfaces.

By applying mathematical model it is possible to synthesize interferometric patterns. Interferogram view depends on light source parameters and surface topology. In the Fig. 2 there are interferograms of tilted (a) and spherical (b) surfaces for light of central wavelength $\lambda_0 = 620$ nm and bandwidth $\Delta\lambda = 52$ nm. Interferograms contain 1000 pixels on vertical and horizontal axes.

Synthesis of surfaces, interferograms and data processing with the aim of reconstruction of surface profile is done in MatLab package, because it contains developed library of functions which are necessary to conduct researches.

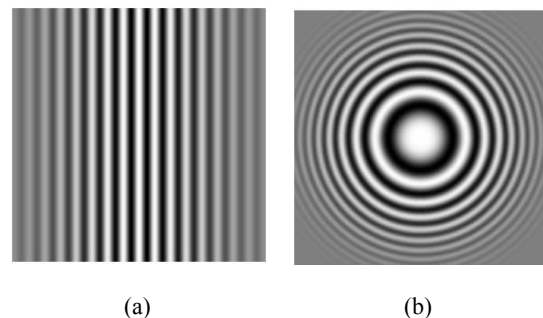


Fig. 2. White light interferograms of tilted (a), and spherical (b) surfaces.

Interferometric pattern is created as set of pixels of different intensity and every line of interferogram can be considered as discrete signal $I(n)$. Dependence of intensity signal on sample number n is different significantly for flat and spherical surfaces (Fig. 3).

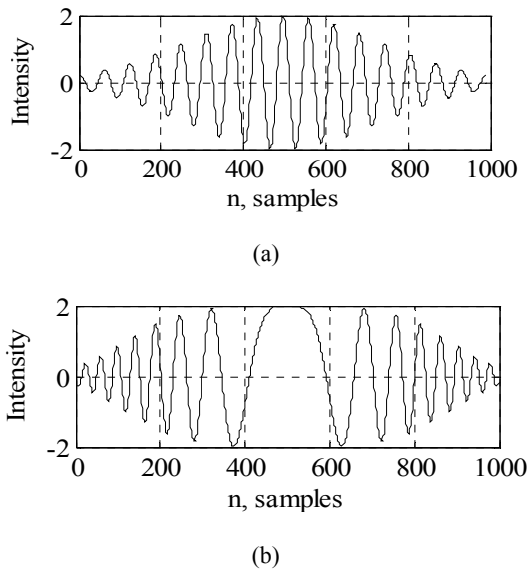


Fig. 3. Interferogram central row of tilted (a), and spherical (b) surfaces.

In contrast to this, the dependence between intensity signal I and optical path difference T in accordance with (1) is identical regardless of researched surfaces form. This aspect of invariance is put in the basis of developed method of segmental approximation.

6. Segmental Approximation Method

Since mentioned above the intensity signal as function of optical path difference is invariant to the profile of researched surface. So the shape of the intensity signal obtained on the linear surface can be transferred on spherical surface and vice versa on conditions that values of optical path difference are close.

If interferogram segment is approximated by polynomial:

$$\tilde{T} = \sum_{m=0}^M \alpha^m T^m, \tag{3}$$

so reconstruction of surface profile demands search of polynomial roots that is calculating-complicated task.

However the reconstruction is sufficiently simplified under application of the function which is reciprocal to $I(T)$ (Fig. 4). Determination of informative parameter T demands approximation function value computing:

$$\tilde{T} = \sum_{n=0}^N a^n I^n \tag{4}$$

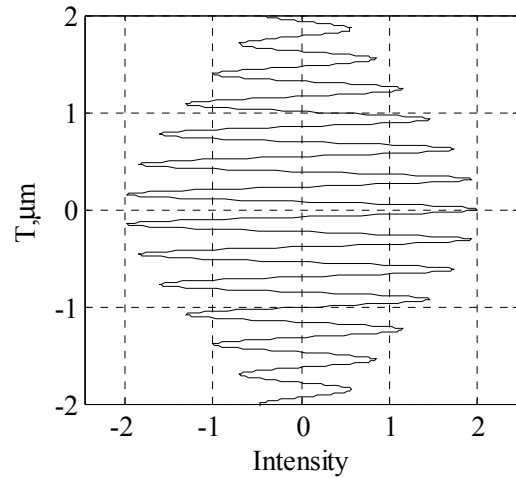


Fig. 4. Graph of informative parameter T on interferogram intensity I .

This approach enables to approximate profile fragment on calibration surface (with known parameters) and further to apply approximating results for any other surface. In practice it looks like as calibration of interferometer measuring channel, therefore light source parameters have to be identical at calibrating and measuring stages.

Given in the Fig. 4 function is multivalued with variable area of T dimensions at different segments. These conditions complicate the problem of polynomial approximation of $T(I)$ function. Therefore approximation has to be performed for every segment of $T(I)$ function. Segment is a stretch of function within change of I argument values. $T(I)$ function segmentation is conveniently to bring to search of local extremes of its reciprocal version, i.e. to intensity of registered signal (Fig. 5).

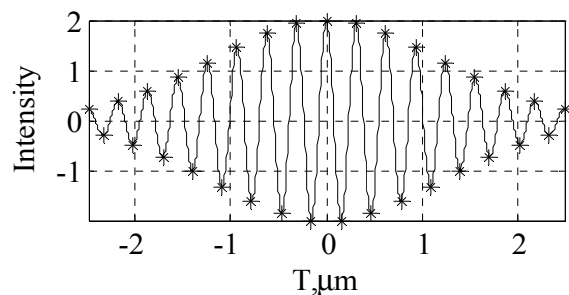


Fig. 5. Signal intensity segmentation in the space.

At every segment the optical path difference is approximated separately by algebraic polynomial with help of MatLab package:

$$\tilde{T} = a_0 + a_1 * I_C + a_2 * I_C^2 + \dots + a_N * I_C^N, \quad (5)$$

where I_C is signal intensity on calibration stage; $a_0 \dots a_N$ are the polynomial coefficients.

Polynomial coefficients are determined from minimum condition of root-mean-square error of approximation:

$$\varepsilon_A^2 = \min \sum_{k=1}^K (T_k - \tilde{T}_k)^2, \quad (6)$$

where k is a number of signal samples.

Basing on invariance of intensity signal concerning optical path difference, profile of researched surface can be approximated by polynomial with coefficients determined during calibration:

$$T = a'_0 + a'_1 I + a'_2 I^2 + \dots + a'_N I^N, \quad (7)$$

where I is the signal intensity of investigated surface; $a'_0 \dots a'_N$ are the polynomial coefficients obtained in calibration step.

Coefficients values of approximating polynomial depend on intensity signal swing. As confirmation the coefficients of polynomial of 3rd degree for segments 1, 2, 15 and 16 are given in Table 1 received by calibration on the tilted surface (Fig. 1(a)).

Table 1. Coefficients values of approximating polynomials in different segments.

Segment	a ₀ , μm	a ₁ , μm/kd	a ₂ , μm/kd ²	a ₃ , μm/kd ³
1	-2.4	-0.17	-0.2	-1,75
2	-2.25	0.13	-0.11	0.81
15	-0.23	-0.02	-3,96·10 ⁻⁴	-0.004
16	-0.08	0.02	-1,28·10 ⁻⁴	0.0038

This condition makes to select the nearest segment by swing from set of calibrating segments. The criterion for selection is the coverage of analyzing surface segment by calibration one. The simplest selection algorithm is the comparison of extreme values of the analyzed segment with a set of calibration values towards the growth of their swing.

Thus surface reconstruction method by segmental approximation consists of two stages: calibration and, properly, reconstruction.

The interferogram, obtained for surface with known parameters, is registered at calibration of interferometer measuring channel. Then segmentation of received interferogram is performed and polynomial coefficients for every segment are determined by (5).

Reconstruction stage includes the next steps:

- Sownloading of researched surface interferogram data;

- Segmentation of researched interferogram and searching identical “calibration” segment;
- Informative T parameter computing by (7) for every segment;
- Visualization of the reconstructed surface.

7. Verification and Analysis of Results

The methodology of accuracy research envisages synthesis of tilted and spherical surfaces (Fig. 1), simulation of interferogram (Fig. 2) on the basis of mathematical model (1), and surface reconstruction of the basis of developed method. For purpose of deep analysis of method performance the surface reconstruction accuracy was studied on the basis of some lines data. So far as in contrast to tilted surface, the spherical one depends on coordinate y (line number), and research concerned the central row No. 500 and remote from center row No. 150.

To estimate accuracy of reconstruction, the conventional error and root-mean-square conventional error are determined by equations:

$$\gamma(T) = \frac{|T_{rec} - T_{origin}|}{\max(T_{origin}) - \min(T_{origin})} \cdot 100\%, \quad (8)$$

$$\sigma = \frac{\sqrt{\sum_{i=1}^N [T_{rec}(i) - T_{origin}(i)]^2}}{N \cdot [\max(T_{origin}) - \min(T_{origin})]} \cdot 100\%, \quad (9)$$

where $T_{rec}(i)$ is the height of reconstructed surface at the point i ; $T_{origin}(i)$ is the height of original surface at the point i ; N is a number of samples.

The conventional error of tilted surface profile reconstruction is given in Fig. 6.

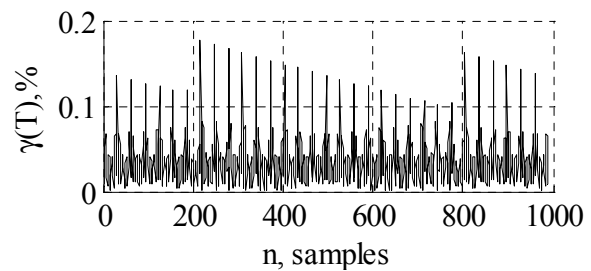


Fig. 6. Conventional error of tilted surface profile reconstruction.

As shown, the reconstruction maximum error doesn't exceed 0.2 %. Error graph is inherent in periodical character with brightly identified spurs. Maximum errors are observed on the borders of segments which are specified by deviation of approximating polynomial from real interferogram. Root-mean-square conventional error is equal to 0.05 %.

There are profile reconstruction conventional errors of spherical surface for central row No. 500 and remote from the center row No. 150 in Fig. 7.

The error character is not periodic for spherical surface, as continuance of interferogram segments of spherical surface is increasing with approaching to the center. Maximum values of conventional error do not exceed 1 %, and root-mean-square conventional error is 0.2 % for row No. 500 and 0.18 % for row No. 150.

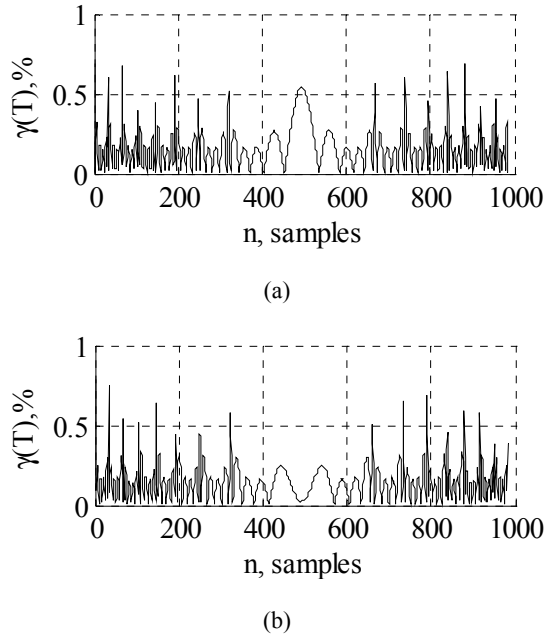


Fig. 7. Conventional error of spherical surface profile reconstruction for rows No. 500 (a) and No. 150 (b).

So far as the source of errors is discrepancy between real interferogram and approximation polynomial, especially on the borders of segments, it was studied the possibility of improvement of reconstruction accuracy by increase of approximation degree.

With increase of polynomial degree the character of errors is not significantly changed; therefore only numerical values of errors are given for linear and spherical surfaces on condition of the use of approximation polynomials of 3, 5 and 15 degrees. Table 2 presents the maximum conventional errors of reconstruction, and Table 3 describes their root-mean-square values.

Table 2. Maximum conventional errors of reconstruction depending on the polynomial degree.

Polynomial degree	$\gamma(T)$, % tilted surface	$\gamma(T)$, % spherical 500 row	$\gamma(T)$, % spherical 150 row
3	0.17	0.69	0.78
5	0.12	0.5	0.57
15	0.06	0.28	0.32

Table 3. Root-mean-square conventional errors of reconstruction depending on the polynomial degree.

Polynomial degree	σ , % tilted surface	σ , % spherical 500 row	σ , % spherical 150 row
3	0.05	0.2	0.18
5	0.03	0.12	0.11
15	0.01	0.03	0.04

Research results have demonstrated that the increase of approximation polynomial degree almost twice and in five times does not adequately improve the reconstruction accuracy.

8. Conclusions

1. Proposed method of segmental polynomial approximation based on invariance of signal intensity of white-light interferogram from optical path difference, is applicable for surface reconstruction at complicated and non-stationary surface topology.

2. The method is computationally simple since 3rd degree polynomial approximation of interferogram segments is applied. It enables its implementation into computing facilities of limited power, f.i., in portable profilometers and embedded units.


3. Metrological properties of proposed method that have been studied on synthesizing surfaces, ascertained that boundary conventional error of reconstruction of tilted surface doesn't exceed 0.2 %, and root-mean-square conventional error is ~ 0.05 %. Similar results are obtained for spherical surface, whose boundary conventional error rises to ~ 1 %, and root-mean-square conventional error to 0.2 %.

References

- [1]. K. Totsu, Y. Haga, *et al.*, 125 mm diameter fiber-optic pressure sensor system using spectrometer-based white light interferometry with high-speed wavelength tracking, in *Proceedings of the 3rd IEEE/EMBS Special Topic Conference on Microtechnologies in Medicine and Biology*, Kahuku, Oahu, Hawaii, 12-15 May 2005, pp. 170-173.
- [2]. K. Schwenzer-Zimmerer, J. Haberstock, 3D Surface Measurement for Medical Application — Technical Comparison of Two Established Industrial Surface Scanning Systems, *Journal of Medical Systems*, Vol. 32, Issue 1, 2008, pp. 59-64.
- [3]. W. Cong-Fei, W. Guang-Long, *et al.*, The signal interrogation technology of MEMS optical fiber pressure sensor, in *Proceedings of the International Conference on Information and Automation*, China, Zhuhai/Macau, 22 -25 June 2009, pp. 1285-1288.
- [4]. K. Kitagawa, 3D Profiling of a Transparent Film using White-Light Interferometry, in *Proceedings of the SICE Annual Conference*, Japan, Sapporo, Vol. 1, 4-6 August 2004, pp. 585-590.

- [5]. W. J. Bock, W. Urbanczyk, Coherence multiplexing of fiber-optic pressure and temperature sensors based on highly birefringent fibers, *IEEE Transactions on Instrumentation and Measurement*, Vol. 49, No. 2, April 2000, pp. 392-397.
- [6]. R. Leach, Optical Measurement of Surface Topography, R. Leach (ed.), Chapter 8, *Springer-Verlag*, Berlin, Germany, 2011, pp. 167-186.
- [7]. P. Hariharan, Basics of Interferometry, 2nd ed., *Elsevier Inc.*, 2007.
- [8]. J. C. Wyant, White light interferometry, in *Proceedings of the SPIE*, Vol. 4737, 2002, pp. 98-107.
- [9]. D. Apostol, V. Damian, P. C. Logofatu, Nanometrology of Microsystems, *Interferometry/Romanian Reports in Physics*, Vol. 60, No. 3, 2008, pp. 815-828.
- [10]. T. Guo, S. Wang, D. J. Dorantes-Gonzalez, J. Chen, X. Fu, X. Hu, Development of a Hybrid Atomic Force Microscopic Measurement System Combined with White Light Scanning Interferometry, *Sensors*, Vol. 12, No. 1, 2012, pp. 175-188.
- [11]. R. Cincio, W. Kacalak, C. Lukianowicz, System Talysurf CCI 6000 – methodic of analysis surface feature with using TalyMap Platinum, *Pomiary, Automatyka, Kontrola*, Vol. 54, No. 4, 2008, pp. 187-191 (in Polish).
- [12]. The Online Industrial Exhibition. Taylor Hobson Precision, Talysurf CCI 6000. The world's highest resolution automated optical 3D profiler, 2005. <http://pdf.directindustry.com/pdf/taylor-hobson/talysurf-cci-6000/7159-132100.html>
- [13]. Th. Seiffert, Schnelle Signalvorverarbeitung in der Weißlichtinterferometrie durch nichtlineare Signalaufnahme, in *DGaO-Proceedings*, Stuttgart, 2004.
- [14]. L. Mingzhou, Development of fringe analysis techniques in white light interferometry for micro-component measurement, Ph.D. Thesis, *National University of Singapore*, 2008.
- [15]. H. Abdul-Rahman, Three-dimensional Fourier fringe analysis and phase unwrapping, *Ph.D. Thesis*, *Liverpool John Moores University*, 2007.
- [16]. H. M. Muhamedsalih, Investigation of wavelength scanning interferometry for embedded metrology, Ph.D. Thesis, *University of Huddersfield*, 2013.
- [17]. B. Stadnyk, E. Manske, A. Khoma, State and prospects of computerized systems monitoring the topology of surfaces, based on white light interferometry, *Computational Problems of Electrical Engineering*, Vol. 4, No. 1, 2014, pp. 75-80.
- [18]. V. Heikkinen, R. Kurppa, *et al.*, Quality control of ultrasonic bonding tools using a scanning white light interferometer, in *Proceedings of the IEEE International Ultrasonics Symposium*, 2010, pp. 1428-1430.

2015 Copyright ©, International Frequency Sensor Association (IFSA) Publishing, S. L. All rights reserved. (<http://www.sensorsportal.com>)



Handbook of Laboratory Measurements and Instrumentation

Maria Teresa Restivo
Fernando Gomes de Almeida
Maria de Fátima Chouzal
Joaquim Gabriel Mendes
António Mendes Lopes

The Handbook of Laboratory Measurements and Instrumentation presents experimental and laboratory activities with an approach as close as possible to reality, even offering remote access to experiments, providing to the reader an excellent tool for learning laboratory techniques and methodologies. Book includes dozens of videos, animations and simulations following each of chapters. It makes the title very valued and different from existing books on measurements and instrumentation.

IFSA
International Frequency Sensor Association Publishing

Order online:
http://www.sensorsportal.com/HTML/BOOKSTORE/Handbook_of_Measurements.htm